HHS Public Access

Author manuscript

Biomaterials. Author manuscript; available in PMC 2016 February 01.

Published in final edited form as:

Biomaterials. 2014 January ; 35(3): 949–960. doi:10.1016/j.biomaterials.2013.10.036.

Janus magnetic cellular spheroids for vascular tissue engineering

Brandon M. Mattix[a,1], **Timothy R. Olsen**[a,1], **Megan Casco**[a,1], **Laura Reese**[a,1], **John T. Poole**[a,1], **Jing Zhang**[b], **Richard P. Visconti**[b], **Agneta Simionescu**[a,1], **Dan T. Simionescu**[a,1], and **Frank Alexis**[a,c,*]

[a]Department of Bioengineering, Clemson University, 301 Rhodes Research Center, Clemson, SC 29634, USA

[b]Department of Regenerative Medicine and Cell Biology, Medical University of South Carolina, 173 Ashley Avenue – BSB 601, Charleston, SC 29425, USA

[c]Institute of Biological Interfaces of Engineering, 401-2 Rhodes Engineering Research Center, Clemson, SC 29634, USA

Abstract

Cell aggregates, or spheroids, have been used as building blocks to fabricate scaffold-free tissues that can closely mimic the native three-dimensional *in vivo* environment for broad applications including regenerative medicine and high throughput testing of drugs. The incorporation of magnetic nanoparticles (MNPs) into spheroids permits the manipulation of spheroids into desired shapes, patterns, and tissues using magnetic forces. Current strategies incorporating MNPs often involve cellular uptake, and should therefore be avoided because it induces adverse effects on cell activity, viability, and phenotype. Here, we report a Janus structure of magnetic cellular spheroids (JMCS) with spatial control of MNPs to form two distinct domains: cells and extracellular MNPs. This separation of cells and MNPs within magnetic cellular spheroids was successfully incorporated into cellular spheroids with various cellular and extracellular compositions and contents. The amount of cells that internalized MNPs was quantified and showed that JMCSs resulted in significantly lower internalization (35%) compared to uptake spheroids (83%, $p < 0.05$). Furthermore, the addition of MNPs to cellular spheroids using the Janus method has no adverse effects on cellular viability up to seven weeks, with spheroids maintaining at least 82% viability over 7 weeks when compared to control spheroids without MNPs. By safely incorporating MNPs into cellular spheroids, results demonstrated that JMCSs were capable of magnetic manipulation, and that magnetic forces used during magnetic force assembly mediate fusion into controlled patterns and complex tissues. Finally, JMCSs were assembled and fused into a vascular tissue construct 5 mm in diameter using magnetic force assembly.

Keywords

Tissue engineering; Magnetic nanoparticles; Iron oxide; Spheroids; Tissue fusion

[*]Corresponding author. 301 Rhodes Research Center, Department of Bioengineering, Clemson University, Clemson, SC 29634, USA. Fax: +1 864 656 4466. falexis@clemson.edu (F. Alexis).

[1]Fax: +1 864 656 4466.

1. Introduction

Three dimensional cell cultures, or spheroids, have been investigated as tissue engineered building blocks due to their ability to mimic the native cellular and extracellular matrix (ECM) environment. It has been established that cellular spheroids fuse together when placed in direct contact with one another, but a method is required to hold them in place to promote their fusion. This can be achieved using a variety of techniques, including direct seeding into a mold [1,2], printing into hydrogel or biopaper [3–5], surface patterning to promote adhesion [6–9], or patterning mediated by magnetic forces [10–16]. By tailoring and controlling interaction at a sub-cellular level, nanotechnology can be used to improve biocompatibility, tissue integration, and assembly of complex tissues or scaffolds [9,17,18]. A variety of methods that utilize internalization of MNPs into cells have been investigated to integrate MNPs with tissue engineering, including MNP conjugation/binding to the cell [12,16,19], cellular internalization [20–23], and mixing MNPs within the ECM [10,20,24]. However, all of these approaches are limited to short-term studies due adverse effects attributed to MNP internalization into cells. Therefore, there is a need to limit MNP and cell interaction in tissue engineering strategies.

Here, we report a technique to incorporate MNPs into cellular spheroids which avoids adverse effects related to MNP internalization on cell viability and phenotype. This approach goes beyond current MNP strategies by reducing MNP interactions with cells while still allowing for magnetic manipulation, thereby avoiding adverse effects related to MNP internalization [10,11,19,23,25]. These structures possess two segregated domains, one composed of cells and the other of extracellular MNPs to form a Janus magnetic cellular spheroid (JMCS, Fig. 1a). Experiments were performed to evaluate the effect of MNP interaction on cell viability, phenotype, magnetic patterning and fusion, and assembly into complex tissue constructs. The ultimate goal is to evaluate the use of magnetic cellular spheroids as building blocks for tissue engineering, with future broad use in tissue engineering applications, high throughput drug screening, and cellular interactions.

2. Materials & methods

2.1. Statistical analysis

All statistical analysis was performed using a two-tailed *t*-test with at least three repeats each. Statistical significance was set at $p < 0.05$. Error bars on graphs represent the standard deviation from the mean.

2.2. Cell culture

Primary rat aortic smooth muscle cells (SMCs), primary rat aortic fibroblasts (FBs), and human adipose-derived stem cells (ADCSs, Lonza) were used for all studies. All cells were cultured in monolayer cultures at 37 °C and 5% of CO_2 until spheroid assembly. SMCs were cultured using Dulbeco's Modified Eagle Medium:F-12 (ATCC, 1:1, DMEM:F-12) supplemented with 10% fetal bovine serum (Atlanta Biologics) and 1% penicillin-streptomycin-amphotericin (MediaTech, Inc.). FBs were cultured using Dulbeco's Modified Eagle Medium supplemented with 10% fetal bovine serum and 1% penicillin–streptomycin–

amphotericin. ADSCs were cultured using adiposed-dervied stem cell basal medium (Lonza) supplemented with 10% fetal bovine serum, 1% L-glutamine (Lonza), and 0.1% gentamicin–amphotericin B (GA-1000, Lonza).

2.3. Spheroid assembly

To assemble JMCSs, equal volumes of solutions containing suspended iron oxide MNPs (Fe_3O_4, 20–30 nm, SkySpring Nanomaterials, Inc.), collagen (Bovine, Type I, Life Technologies), and cells in cell culture media were combined and dispensed using a hanging drop method into 15 μL droplets. Samples were inverted and incubated at 37 °C with 5% CO_2 for three days prior to use to allow for spheroid assembly. Unless otherwise noted, all spheroids were analyzed after three days in hanging drop and assembled using SMCs with 300 μg/mL MNPs (4.5 mg MNP per spheroid), 20,000 cells per spheroid, and 17 μg/mL collagen (0.255 ug collagen per spheroid). To assemble uptake MNP spheroids, a monolayer cell culture flask (~90% confluence) was incubated with MNP-containing cell culture media (300 μg/mL) for 24 h. The bottom of culture flasks was covered with square magnets (K&J Magnetics, Inc., 12.7 × 12.7 mm, 1.6 mm thick, vendor calculated pull force = 3.59 lbs) to promote MNP internalization into cells. Media solutions containing MNPs were sonicated prior to addition to cells. After incubation, cells were washed 5× to remove free MNPs, trypsinized (0.25%, Thermo Scientific), collected, and placed on a magnetic wash tool and allowed to sit for 5 min. The supernatant was discarded and remaining magnetically attracted cells suspended in fresh media. Solutions of magnetically attracted cells and collagen were combined and dispensed using a hanging drop method as mentioned previously. Collagen was prepared according to manufacturer recommendations and kept on ice prior to use for all samples. MNPs were washed three times with a magnetic wash tool prior to use to remove byproducts. To assemble dispersed spheroids, equal volumes of solutions containing sonicated suspended iron oxide (300 μg/mL) MNPs (Fe_3O_4, 20–30 nm, SkySpring Nanomaterials, Inc.), collagen (Bovine, Type I, Life Technologies), and cells in cell culture media were combined and dispensed using a hanging drop method into 15 μL droplets.

2.4. Histology

JMCSs were processed and sectioned via standard paraffin sectioning techniques. Briefly, spheroids were fixed overnight with Z-Fix (buffered zinc formalin, Anatech Ltd.) and dehydrated using ethanol and xylene prior to paraffin embedding. 5 μm thick sections were stained using hemotoxylin and eosin (H&E) and Masson's Trichrome (Poly Scientific). JMCSs were collected and analyzed after three days of assembly in hanging drop.

2.5. Viability

Presto Blue (Life Technologies) and MTT (Sigma) cell viability assays were performed using spheroids composed of primary rat aortic smooth muscle cells, primary rat aortic fibroblasts, and human adipose-derived stem cells to quantify cell viability (at least 3 repeats per sample). Spheroids were first dissociated via incubation with collagenase (80 min, Collagenase Type IV, Life Technologies), followed by incubation with trypsin (10 min). Spheroids were centrifuged and physically dissociated, then allowed to adhere overnight on a well plate. Viability was also qualitatively analyzed for JMCSs and No MNP Controls

following manufacturer's specifications using simultaneous live/dead fluorescent staining and imaging using Calcein, AM (live) and ethidium homodimer-1 (EthD-1, dead). Spheroids were stained, fixed using Z-fix, and imaged using a Nikon Eclipse Ti confocal microscope. All JMCSs were collected and analyzed after three days of assembly in hanging drop except those used for long-term viability studies. Spheroids used for long term viability studies were cultured in non-treated well plates with media changes every other day.

2.6. Quantification of MNP internalization

Cellular spheroids composed of primary rat aortic smooth muscle cells (25, Janus and Uptake) were dissociated via collagenase and trypsin as previously described. Dissociated samples were suspended in 1 mL fresh media and placed on a magnetic wash tool for 5 min. The supernatant was collected, and the remaining cells (magnetically attracted) suspended in 1 mL fresh media. The amounts of cells in the supernatant and magnet solution were quantified using a hemocytometer. Spheroids were collected and analyzed after three days of assembly in hanging drop.

2.7. Phenotype analysis

Flow cytometric analyses were conducted using a Beckman Coulter Astrios cell sorter. Spheroids were dissociated (collagenase and trypsin), filtered, suspended in CytoFix/Cytoperm buffer, and incubated with primary antibodies including smooth muscle α-actin (SMAA) conjugated with Cy3 (SigmaeAldrich), smooth muscle 22 (SM22, Abcam), and smooth muscle myosin heavy chain (SMHC, Biomedical Technologies, Inc.). Rabbit IgG-Cy5 (Jackson ImmunoResearch) was used as a secondary antibody. Spheroids were collected and analyzed after three days of assembly in hanging drop.

Immunofluorescence microscopy was used to qualitatively confirm SMC phenotype expression within samples. First, OCT embedded histology sections (5 μm thick) were collected and cleared via two washes (5 min) in PBS and 1 wash in water. Samples were circled with a diamond tip pen. Samples were treated with a 0.1% Triton X-100 to permeabilize samples (10 min). Slides were washed 3× with water (5 min), followed by a 30 min incubation with Background Buster (Innovex Biosciences). Next, samples were washed 2×water and 1× PBS. Once samples were prepped, they were incubated with primary antibodies overnight at 4 °C in a humid chamber. Samples were washed 3× PBS, followed by incubation with secondary antibodies for 1 h at room temperature. As a control, samples were incubated with just the secondary antibody to ensure controlled binding was occurring. Finally, samples were washed 3× PBS followed by incubation with Hoechst 33342 to stain for nuclei (10 min, room temperature). Samples were washed 3× PBS and cover slipped, and fluorescently imaged for SMHC and SM22 (FITC, Ex/Em 492/520), SMAA (Cy3, Ex/Em 552/570), and nuclei (Hoescht 33342, Ex/Em 343/483). Results were analyzed and compared to samples containing no MNPs to determine the effects of MNP integration on SMC phenotype marker expression. Three samples of each formulation were analyzed to confirm that results were consistent. Spheroids were collected and analyzed after three days of assembly in hanging drop.

2.8. Magnetic patterning

JMCSs and uptake spheroids, composed of primary rat aortic smooth muscle cells, were patterned into various shapes using magnetic force assembly. Commercial magnets (SuperMagnetMan, Birmingham, AL) of various shapes and strengths were applied to the bottom of glass chamber slides containing coverglass bottoms and maintained for four days. All shapes were allowed to fuse for four days with the magnet in place, with changes in cell culture media every other day. Magnets were removed on the fourth day, and fused tissues were immediately imaged using a Nikon AZ100 multizoom microscope. Small rings were assembled using ring magnets (2 mm OD, 1 mm ID, 1 mm thick, vendor calculated pull force = 0.16 lbs). Medium and large rings were assembled using aligned cylinder magnets in a circular pattern (2.5 mm diameter, 5 mm length, pull force = 1.8 lbs). Square shapes were patterned using aligned cylinder magnets in a square pattern (2.5 mm diameter, 2.5 mm length, pull force = 1.57 lbs). The Clemson University Tiger Paw shape was assembled using custom cut magnetic strips.

2.9. Tissue fusion

Capillary tubes (500 mm diameter, CTechGlass, CT95-02) were used to study the influence of magnetic forces on cellular spheroid fusion. JMCSs (primary rat aortic SMCs), were assembled and placed into a capillary tube full of cell culture media. Spheroid filled capillary tubes were placed upright into a 0.65 mL polypropylene conical tube with cell culture media to allow spheroids to settle to the bottom. Samples were exposed to magnetic forces via placement of a square magnet below sample containers (K&J Magnetics, Inc., B881). Spheroids were left in capillary tubes for 48 h prior to imaging analysis. Samples in capillary tubes were imaged using an AMG EVOS fl Digital Inverted Microscope. Spheroids were first imaged in the capillary tubes and then removed to be imaged outside the capillary tubes. At least three repeats were used for each condition to confirm repeatability. Fluorescently labeled spheroids were stained using a Vybrant® CFDA SE Cell Tracer Kit (green, Life Technologies) and PKH26 Red Fluorescent Cell Linker Kit (red, Sigma). Stains were performed according to manufacturer protocols. Fluorescent images were captured using a Nikon Ti Eclipse microscope.

Spheroid fusion was also analyzed by tracking the fusion of spheroids into a ring. Ring magnets were commercially purchased (2 mm OD, 1 mm ID, 1 mm thick, Super Magnet Man). Twenty five individual JMCS SMC spheroids (17 μg/mL collagen, 300 μg/mL MNPs, 20,000 cells) were patterned around the ring pattern in a monolayer formation (Fig. 8a). Magnets were kept in place for 48 h and then removed, followed by imaging with a Nikon AZ100 multizoom microscope at respective time points. Magnet strength was varied by increasing the distance of the ring magnet away from the magnetic cellular spheroids (coverglass spacers placed on the bottom of the chamber slides). Four measurements for each diameter (inner and outer) were recorded and averaged at each time point. Samples were normalized with themselves (based on initial inner and outer diameter measurements at 48 h), as each sample was analyzed as the percent-initial diameter. At least three repeats were performed for each sample.

Furthermore, spheroid fusion was studied using ring molds as a model. Molds were cut from a sheet of silicone and uniformly fabricated to leave a ring mold for spheroids to be seeded into. Prior to use, molds were sterilized and fixed to petri dishes. Approximately 500 JMCSs (primary rat aortic SMCs) were seeded into each ring mold and chambers filled with cell culture media. A magnet was fixed to the bottom of the petri dishes containing the molds filled with JMCSs, while no magnets were used with MNP-free control samples. Samples were imaged using an AMG EVOS fl Digital Inverted Microscope immediately after seeding and again after 48 h. At the 48 h time point, a Nikon AZ100 multizoom microscope was used to image the JMCS ring fusion mediated by magnetic forces.

2.10. Fabrication of vascular tissue construct

Using a polystyrene petri dish, a long rod magnet (45 mm) composed of stacked cylinder magnets (2.5 mm diameter, 5 mm length, pull force = 1.8 lbs) was secured to the bottom side of the petri dish. A glass slide was placed on the top surface of the petri dish to promote spheroid fusion. Thousands of JMCSs were added to the media-filled petri dish and assembled on top of the magnetic template (Supplementary Fig. S1). Care was taken to seed JMCSs evenly along the pattern. Magnetic cellular strips were incubated and allowed to fuse over 4 days, with media changes every other day. Next, magnetic cellular strips were wrapped around a silicone tube (5 mm OD, 2.5 mm ID, Cole–Parmer) containing a magnet (2.5 mm diameter, 5 mm length, pull force = 1.8 lbs) within its lumen to form a tissue tube. To avoid oxidation of the magnet by culture media, the ends of the silicone tube were plugged with silicone rubber. The silicone tube was rolled over the top of the cellular strip to effectively wrap the strip around the tube. Samples were incubated in culture media to allow more fusion for 6 additional days. To assemble bilayer tubes, two separate magnetic cellular strips were assembled and wrapped around the same silicone mandrel in sequential order based on the desired spatial orientation. This same technique was applied to assemble a vascular tissue construct. Single layer tissue tubes were assembled using SMC JMCSs (2000). Bilayer tissue tubes were assembled using an internal strip of SMC JMCSs (2000) and an external layer of FB JMCSs (2000). Finally, a vascular tissue construct was assembled using an internal strip of EC JMCSs (1500), medial strip of SMCs (1500), and external strip of FBs (1500). All JMCSs were composed of 20,000 cells, with 0.24 mg/mL collagen, and 0.3 mg/mL iron oxide MNPs.

To study the assembly of the vascular tissue construct, three separate trilayer tubes were assembled. Each trilayer tube contained three different cell types (FBs, SMCs, ECs), with one cell type fluorescently labeled in each tube. Cells were fluorescently labeled in suspension prior to spheroid assembly using a Vybrant CFDA SE Cell Tracer Kit (Life Technologies). JMCSs were assembled for three days in a modified hanging drop as previously described, with all JMCSs composed of 20,000 cells, 0.24 mg/mL collagen, and 0.3 mg/mL iron oxide MNPs. Trilayer tissue tubes were assembled as previously described (1500 spheroids per tissue strip) via sequential wrapping. However, fusion times were decreased in order to maintain fluorescent signal for imaging. Spheroids were seeded onto a tissue strip and allowed to fuse for 24 h (compared to 4 days as previously described), then wrapped around a silicone tube and allowed to fuse for an additional 24 h (compared to 6 days as previously described). Samples were fixed overnight, then histologically processed

and sectioned the following day. Tissue sections were permeabilized with Triton-X and stained with DAPI to visualize nuclei. Samples were fluorescently imaged using a Nikon Ti Eclipse microscope.

3. Results

3.1. Histology

To analyze the spatial localization of MNPs and cells within JMCSs, samples with Janus structures were histologically sectioned and stained using Masson's Trichrome (Fig. 1b) and hematoxylin and eosin (H&E, Fig. 1f–h). Samples containing increasing concentrations of MNPs showed localization of MNPs and cells into distinct regions. A spheroid without MNPs was histologically stained with hematoxylin and eosin (H&E, Fig. 1c). Dispersed and Uptake spheroids (300 μg/mL MNPs) (Fig. 1g–h) were also stained with hematoxylin and eosin.

3.2. Effect of MNP internalization

JMCSs were compared to Uptake MNP spheroids to determine if the Janus structure improved upon MNP interaction with cells within cellular spheroids. The amount of cells that internalized MNPs was quantified (average) and showed that JMCSs resulted in significantly lower internalization (35%) compared to uptake spheroids (83%, $p < 0.05$, Fig. 2a). Next, cellular viability using both Janus and Uptake cellular spheroids was analyzed up to one week to determine their capacity for tissue engineering applications which involve prolonged interaction between MNPs and cells. A viability analysis (300 μg/mL MNP) showed that JMCSs maintained high viability when compared to control spheroids without MNPs, while uptake spheroids resulted in lower viability at Days 3 and 7 ($p < 0.05$, Fig. 2b). Additionally, the use of JMCSs was compared to conventional uptake magnetic cellular spheroids for tissue assembly (Fig. 2c). Spheroids were assembled onto a magnetic pattern and allowed to fuse for 48 h, at which point the magnet was removed (Fig. 2c, before), and the rings were physically transferred to new a chamber. Fused rings composed of Janus spheroids maintained tissue structure in contrast to those composed of uptake spheroids, which dissociated upon handling (Fig. 2c, after). This dissociation of tissue composed of uptake spheroids could be due to decreased cell viability as shown in Fig. 2b, and therefore tissue integrity. These results confirm that the method used to incorporate MNPs into cellular spheroids is critical in mediating cell fate. Furthermore, the degradation of MNPs within cellular spheroids was analyzed. Results showed that the method used to incorporate MNPs into spheroids was also critical in mediating MNP degradation, as JMCSs demonstrated significantly more MNP degradation (63% iron remaining) compared to Uptake MNP spheroids (88% iron remaining, $p < 0.05$) after 21 days (Fig. 2d).

3.3. Phenotype analysis

Next, studies analyzed samples to determine any adverse effects of MNPs on cell phenotype expression. Flow cytometric analysis was performed on cells from spheroids (control with no MNPs, Janus MNPs, and Uptake MNPs) to determine the percentage expression of three SMC markers: smooth muscle α-actin (SMAA), smooth muscle 22 (SM22), and smooth muscle myosin heavy chain at Day 3 (SMHC, Fig. 2e). Compared to no MNP control

spheroids, JMCSs and Uptake MNP spheroids maintained equivalent expression of SMAA (99% and 93% respectively, normalized to control). Additionally, high SM22 expression was maintained for Janus spheroids (95%), while uptake spheroids resulted in decreased expression (74%). However, the addition of MNPs using the Janus method did result in a slight decrease in SMHC expression compared to no MNP controls (75%), while Uptake MNP spheroids exhibited a significant decrease in expression (16%). These results were also qualitatively analyzed using immunofluorescence microscopy (Fig. 2f), with a uniform dispersion of markers throughout JMCSs compared to controls without MNPs. These results indicate that the presence of MNPs within Janus spheroids did not affect cell phenotype, compared to spheroids without MNPs as both populations expressed SMC-specific markers at similar levels.

3.4. Viability

To determine the capacity for JMCSs to be utilized across a variety of tissue engineering applications, quantitative and qualitative methods were used to analyze viability using various JMCS formulations. The effect of JMCS composition on cell viability was analyzed by varying: the length of culture (Fig. 3a,b), the type of cells (Fig. 3c), and the amount of cells (Fig. 3d). Cell viability was quantified up to seven weeks, with results demonstrating sustained high viability over the seven weeks compared to cellular spheroids without MNPs (Fig. 3a,b). Statistical analysis on long-term viability samples showed significant differences between samples at Day 3 and 1 Week, but in favor of JMCSs compared to controls (normalized viability greater than 100%). Though a statistically significant difference was noted at 5 Week ($p = 0.01$), this difference disappeared at Week 7. Spheroid viability was also qualitatively assessed at 7 weeks using simultaneous live/dead staining, confirming equivalent expression in spheroids with and without MNPs (Fig. 3b, Day 3 Supplementary Fig. S2). These results confirm the long-term *in vitro* viability of JMCSs. Second, JMCSs were assembled using three different cell types to determine if cell viability was dependent on cell type at Day 3 (Fig. 3c), which could prevent further applications to fabricate multicellular tissues. Compared to samples without MNPs, JMCSs composed of rat aortic smooth muscle cells (SMCs), human adipose-derived stem cells (ADSCs), and rat aortic fibroblasts (FBs) maintained high cell viability. Finally, JMCSs were assembled with increasing number of cells (Fig. 3d). Results demonstrated high cell viability between spheroids containing various cell numbers at Day 3. Viability was also maintained in short term studies with MNP concentrations up to 5 mg/mL (Supplementary Fig. S3).

3.5. Magnetic patterning

Next, studies evaluated the ability of JMCSs to fabricate tailored 3D cell constructs and tissues through a series of experiments utilizing magnetic assembly into a variety of shapes (Fig. 4a–c, e, f). Magnetic force manipulation was used to assemble shapes with varying sizes including rings, a square, and the Clemson University Tiger Paw. Results showed that fused tissues, confirmed by a lack of voids or gaps within tissues, were successfully assembled using a variety of shapes and sizes after four days of fusion using magnetic force assembly. Additionally, viability of fused tissue was confirmed on Day 4 by simultaneous live/dead fluorescent staining that showed no visible signs of decreased viability, suggesting that high viability was maintained throughout tissue fusion (Fig. 4d).

3.6. Fabrication of vascular tissue construct

Next, studies expanded on the assembly of complex tissues using JMCS to assemble a 3D vascular tissue construct. Results demonstrated the ability of individual JMSCs to fuse together into a complex 3D tissue whose assembly is driven by magnetic forces. Using magnetic forces and 2000–4000 JMCSs, spheroids were first magnetically patterned into a cellular strip, fused into a tissue strip (Fig. 5a, b), and wrapped around a tube with a removable magnetic within its lumen (Fig. 5c, d). Finally, the magnet within the lumen was removed, leaving behind a fused tissue tube composed solely of JMCSs (Fig. 5e, f). This method was applied to a variety of JMCS compositions, including varying cells numbers within JMCSs (Fig. 5g, h), cell types (Fig. 5i), and even multicellular bilayered tubes using both SMCs and FBs (Fig. 5j). The use of magnetic force manipulation and patterning allowed for the rapid assembly of a complex tissue tube composed of tailored cell, ECM, and MNP content. The dimensions of the vascular tissue construct are controlled by the silicone tube diameter, cell strip length, and cell strip width. This approach allows for the assembly of a cell-based vascular tissue possessing a similar composition to native vessels by controlling JMCS's cell, ECM, and MNP composition. To understand the effect of collagen content on tissue tube assembly, the mechanical stability of tissue tubes was analyzed. Bilayer tissue tubes were assembled using both high (0.24 mg/mL) and low (0.017 mg/mL) collagen spheroids as previously described. Results showed that upon removal of the tissue tubes from the mandrel after day ten of assembly, low collagen tubes immediately collapsed (Fig. 5k). In contrast, high collagen tissue tubes remained open and patent upon removal from the mandrel. These high collagen tubes were self-retaining and capable of physical manipulation while low collagen tubes were incapable of physical handling. Therefore, due to the immediate collapse and inability for physical handling, low collagen tissue tubes were inadequate as a functional tissue engineered construct.

Complex tissue tubes composed of multiple cell types were assembled to form a functional vascular tissue construct. Using magnetic force assembly, thousands of JMCSs were assembled into a fused vascular tissue construct of 5 mm in diameter. As a proof of concept, a vascular tissue construct mimicking both the spatial composition and content of a small diameter blood vessel was assembled. Results showed that unilayer (SMC only) and bilayer (FB and SMC) tubes were successfully assembled (Supplementary Fig. S4). Ultimately, a vascular tissue construct composed of an internal layer of endothelial cells, medial layer of SMCs, and external layer of FBs was assembled. Cell layers were spatially oriented in this manner to mimic the tunica intima (endothelial cells), tunica media (SMCs) and tunica adventitia (FBs) of native blood vessels. Furthermore, analysis was performed to confirm control over the spatial location of cells within assembled tissues. Three separate vascular tissue constructs were assembled, with one cell type labeled within each tube. Results showed that the spatial location of different cell types could be tailored to mimic the orientation of native vascular tissue layers, confirmed by an external layer of FBs (Fig. 6a), medial layer of SMCs (Fig. 6b), and internal layer of ECs (Fig. 6c). While the thickness of each cell layer is not representative of that found in native tissues, the presented technique for tissue assembly can control the thickness of each cell layer based on the number of spheroids used during assembly.

3.7. Tissue fusion

The assembly of complex 3D tissues using cellular spheroids is heavily reliant upon efficient fusion of spheroids into a single tissue. When placed in contact, cellular spheroids will fuse together, with the tissue contracting into a single tissue construct [26]. To study the effects of magnetic forces on tissue spheroid fusion compared to spheroids without MNPs (control), a silicon ring mold was fabricated and filled with spheroids. When no MNP control spheroids were seeded into the ring molds, minimal fusion was evident after 48 h (Fig. 7a, no MNP controls) as individual spheroids were still visible and the construct dispersed upon handling. However, when JMCSs were seeded into the ring molds and exposed to magnetic forces, results demonstrated that a fused tissue construct had formed after 48 h (Fig. 7a, Janus MNP). To further study the effects of magnetic forces on tissue spheroid fusion, JMCSs were placed into capillary tubes and allowed to fuse with the application of magnetic forces. Capillary tubes were incubated in a vertical position for 48 h to ensure spheroid contact throughout the fusion time. After 48 h, results showed that samples prepared with JMCSs under the influence of magnetic forces produced a fused and cohesive tissue structure (Fig. 7b, capillary tube) that remained fused upon removal from the capillary tube and was capable of physical manipulation, confirming tissue fusion into a homogenous tissue (Fig. 7b, in solution). Furthermore, fluorescent staining of the fused JMCS construct showed that the spatial orientation of the spheroids is maintained within the fused tissue (Fig. 7b, fluorescent). These results show that the application of magnetic forces is critical to accelerate spheroid fusion into complex tissues compared to spheroids without MNPs (control).

Furthermore, studies were performed to determine how other parameters mediate spheroid fusion into complex tissues. Spheroid fusion was first analyzed by tracking the fusion of spheroids into controlled patterns using various JMCS and assembly parameters. Twenty five individual JMCSs were magnetically assembled into a ring and their fusion was tracked (Fig. 8a). Images were taken daily and fusion was tracked by measuring changes in the inner and outer diameters of fused tissue rings. Studies varied the strength of the ring magnet to determine the effect of magnetic forces on JMCS fusion. JMCSs patterned using the weakest magnet (10% of maximum magnetic field) showed an increased rate of contraction of the inner diameter compared to other samples patterned with higher magnetic field strengths (Fig. 8b, c). All samples tested using 10% of the maximum magnetic field collapsed on themselves, leaving behind no inner diameter at late time points. While a reduction in internal diameter was observed when using a high (100%) and medium (25%) magnetic field at the late time points, fully fused rings were not seen. Rings fabricated using high and medium magnets fused into cohesive rings while maintaining their desired final shape. All rings were magnetically assembled into symmetric rings on Day 0 after initial seeding. It was hypothesized that rings patterned using 10% of the maximum magnetic field assembled into more asymmetric rings after 48 h of fusion (with the magnet present) due to the necessity of sufficient magnetic force for effective magnetic patterning and fusion. Results showed that similar to the strength of the magnetic field, lower MNP contents lead to a statistically significant increase in rate of contraction (Supplementary Fig. S5) due to a decrease in the total magnetic field applied to the tissue with lower amounts of MNPs present. Finally, studies analyzed the fusion of JMCSs into a tube by varying the fusion time

(Fig. 8d). Bilayered vascular tissue constructs were assembled and histologically analyzed after four and ten days of assembly. Results showed that fusion time is critical in assembling complex tissues, as samples analyzed at Day 4 still presented individual spheroids within the tissue core. Samples analyzed at Day 10 showed clear fusion of individual JMCSs into a single fused tissue. H&E staining at both time points confirmed the presence of viable cells, as visualized by nuclei throughout the tissues.

4. Discussion

Overall, the concept of using magnetic forces to manipulate cellular spheroids has been shown to be promising as magnetic force assembly allows for scaffold-free immobilization and patterning at a distance [10,11]. However, the advances to integrate MNPs with tissue fabrication have failed due to toxicity related to MNP uptake into cells or adverse affects on cell function and morphology [23,27,28]. Ultimately, a magnetic cellular spheroid structure possessing two segregated domains, one composed of cells and one composed of MNPs, will fully incorporate the positive benefits of using magnetic cellular spheroids to go beyond current approaches. The formation of separate domains reduces the interaction and uptake of MNPs into cells, thereby avoiding any adverse effects while still allowing for magnetic force manipulation.

The ability to magnetically assemble tailored engineered building blocks with controlled cell and ECM compositions provides a capability to assemble tissue structures with tailored compositions. Results confirm that the method used to incorporate MNPs into cellular spheroids is critical, as internalization of MNPs clearly has an effect on the phenotype expression and viability. These results indicate that the presence of MNPs within Janus spheroids did not affect cell phenotype, compared to spheroids without MNPs as both populations expressed SMC-specific markers at similar levels. Although some studies have shown that MNPs have no adverse effects on cell phenotype [24,29], others have demonstrated adverse impact on cell motility, length, and other morphological abnormalities, suggesting that use of MNPs results in altered cell phenotype [27,28]. Consequently, it is critical to prevent MNP interactions with cells for tissue engineering applications. This Janus method for MNP-incorporation is expected to overcome the problems associated with MNP internalization, thereby allowing for more complex and long-term applications using MNPs in tissue engineered constructs.

Compared to top-down tissue engineering approaches, directing tissue assembly with bottom-up approaches has become appealing due to control over construct spatial arrangement. As the bottom-up approach is intrinsically a modular technique, it allows for precise control over the tissue construct microenvironment and the ability to scale fabrication techniques [30,31]. Once factors affecting spheroid assembly and fusion into complex tissues using magnetic forces are understood, these parameters can be customized and applied for the assembly of a variety of engineered tissues types. Cellular spheroids are appealing candidates for the assembly of engineered tissues due to the high cell density within fused tissues. Groups have shown that cell density is critical to fabricating tissue constructs, as higher cell density spheroids have lead to increased viability and metabolic output, compared to lower cell densities [32]. Furthermore, the dramatic reduction in

internal diameter of fused rings has been reported by other groups when analyzing fusion of cellular spheroids, while also showing some slight differences in fusion between different cell lines [33]. However, to our knowledge, mediation of tissue fusion using magnetic forces has not been described, and is possibly due to the changes of surface angle contact between spheroids [26]. Kelm et al. showed that the application of fluid flow to the lumen of the fused tissue led to an increased fusion of assembled spheroids into a tissue tube [2]. The presented results show that by varying the magnetic forces during fusion, fusion of JMCSs into a single fused tissue without fluid flow can be controlled. The dimensions of the vascular tissue construct are controlled by the silicone tube diameter, cell strip length, and cell strip width. Other groups have stacked cell rings into a fused tissue tube, but this technique does not allow complete control of cellular spatial location [34]. These stacked rings techniques only allow spatial control in one direction with alternating cell types during stacking. The presented results demonstrate a method for tissue tube assembly which can control the spatial location of cells from the lumen to the exterior, thereby mimicking a small diameter blood vessel. These results suggest that collagen content plays a critical role for structural support when fabricating complex tissue structures composed of fused spheroids. An advantage of tissue engineering with spheroids is that fusion can occur within days, but the mechanical properties of the tissues tend to be inadequate [35]. The results suggest that collagen can provide a natural scaffold for the fusing tissue at its early stages, which allows the tissues to maintain structure and potentially be handled for introduction into post-processing techniques for maturation [4].

The results also demonstrate the critical effect of magnetic forces for mediating tissue fusion with JMCSs. Conventional nonmagnetic tissue assembly and fabrication methods include cell printing, cell sheet techniques, and patterned molds [4,36–38]. These non-magnetic methods spatially orient the cells into a desired position through passive contact, but do not address active contact mediated by forces. The presented studies using silicone ring molds and capillary tubes highlight the application of magnetic forces in mediating tissue fusion and demonstrate the critical importance of magnetic forces in promoting and accelerating tissue fusion over time, when compared to spheroids without MNP used in molds to fabricate tissues.

Results also confirm control over the spatial location of different spheroids to assemble tailored multicellular tissues. This approach will allow for the assembly of a cell-based vascular tissue possessing a similar composition to native vessels by controlling JMCS’s cell, ECM, and MNP composition. Other groups have demonstrated spatial control of multicellular vascular tissue constructs, but require complex printing equipment for assembly [5]. Additionally, this approach to wrap a magnetic cell sheet around a magnetic mandrel has been previously utilized to assemble multicellular tissue tubes [39]. However, Ito et al. induced internalization of MNPs into cells prior to cell sheet assembly, and will likely encounter adverse effects related to MNP uptake in long-term applications [22,28]. The presented strategy to assemble multicellular vascular tissue constructs demonstrates the critical effect of magnetic forces on fusion to spatially control tissue engineered building blocks into tissue tubes. Furthermore, the use of JMCSs, which have been shown to reduce adverse effects on cell phenotype and viability, are appealing for tissue engineering strategies which require long-term interaction between MNPs and cells.

5. Conclusion

The cytotoxicity and phenotypic analyses showed that the JMCS structure can integrate MNPs with biological structures without compromise to cells, thus extending beyond current approaches using MNPs to engineer heterogeneous constructs composed of multiple cell lines. Due to the requirement of long-term cell and MNP interactions to prepare fully functional complex tissues, it is critical to maintain long-term cell viability and stable phenotype. Results have demonstrated that magnetic forces can be used to successfully assemble and manipulate spheroids into controlled patterns and mediate their fusion over time, a strategy that can be used to assemble larger 3D tissue constructs. These results show that it is critical to control the magnetic forces to mediate fusion of tissues using magnetic cellular spheroids. The ultimate goal of this technology will be the assembly of larger tissue structures using magnetic force assembly, with the additional opportunity to use magnetic forces and manipulation for tissue construct maturation. Future research will entail the fusion mechanisms of magnetic cellular spheroids, cell migration, and production of extracellular matrix.

Supplementary Material

Refer to Web version on PubMed Central for supplementary material.

Acknowledgments

This work was supported by the American Heart Association Beginning Grant in Aid-2BGIA11720004 award to F.A., the SC EPSCoR Grant for Exploratory Academic Research-2012001188 award to F.A., and the NSF/EPSCOR EPS-0447660 award to R.P.V. The authors wish to thank Dr. R. Markwald from the Medical University of South Carolina and Dr. V. Mironov for discussing challenges and innovations in tissue fabrication. We would also like to thank Dr. T. Bruce and the Clemson Light Imaging Facility at Clemson University for technical support with microscopy and Mrs. L. Jenkins for her help with histological techniques.

Appendix A. Supplementary data

Supplementary data related to this article can be found at http://dx.doi.org/10.1016/j.biomaterials.2013.10.036.

References

1. Kelm JM, Djonov V, Ittner LM, Fluri D, Born W, Hoerstrup SP, et al. Design of custom-shaped vascularized tissues using microtissue spheroids as minimal building units. Tissue Eng. 2006; 12:2151–60. [PubMed: 16968156]
2. Kelm JM, Lorber V, Snedeker JG, Schmidt D, Broggini-Tenzer A, Weisstanner M, et al. A novel concept for scaffold-free vessel tissue engineering: self-assembly of microtissue building blocks. J Biotechnol. 2010; 148:46–55. [PubMed: 20223267]
3. Jakab K, Norotte C, Damon B, Marga F, Neagu A, Besch-Williford CL, et al. Tissue engineering by self-assembly of cells printed into topologically defined structures. Tissue Eng Part A. 2008; 14:413–21. [PubMed: 18333793]
4. Jakab K, Norotte C, Marga F, Murphy K, Vunjak-Novakovic G, Forgacs G. Tissue engineering by self-assembly and bio-printing of living cells. Biofabrication. 2010; 2:022001. [PubMed: 20811127]
5. Norotte C, Marga FS, Niklason LE, Forgacs G. Scaffold-free vascular tissue engineering using bioprinting. Biomaterials. 2009; 30:5910–7. [PubMed: 19664819]

6. Fukuda J, Sakai Y, Nakazawa K. Novel hepatocyte culture system developed using microfabrication and collagen/polyethylene glycol microcontact printing. Biomaterials. 2006; 27:1061–70. [PubMed: 16111746]
7. Otsuka H, Hirano A, Nagasaki Y, Okano T, Horiike Y, Kataoka K. Two-dimensional multiarray formation of hepatocyte spheroids on a microfabricated PEG-brush surface. ChemBioChem. 2004; 5:850–5. [PubMed: 15174169]
8. Wan ACA, Ying JY. Nanomaterials for in situ cell delivery and tissue regeneration. Adv Drug Deliv Rev. 2010; 62:731–40. [PubMed: 20156499]
9. Zhang B, Xiao Y, Hsieh A, Thavandiran N, Radisic M. Micro- and nanotechnology in cardiovascular tissue engineering. Nanotechnology. 2011; 22:494003. [PubMed: 22101261]
10. Bratt-Leal A, Kepple KL, Carpenedo RL, Cooke MT, McDevitt TC. Magnetic manipulation and spatial patterning of multi-cellular stem cell aggregates. Integr Biol. 2011; 12:1224–32.
11. Ho VHB, Müller KH, Barcza A, Chen R, Slater NKH. Generation and manipulation of magnetic multicellular spheroids. Biomaterials. 2010; 31:3095–102. [PubMed: 20045553]
12. Lin R-Z, Chu W-C, Chiang C-C, Lai C-H, Chang H-Y. Magnetic reconstruction of three-dimensional tissues from multicellular spheroids. Tissue Eng Part C Methods. 2008; 14:197–205. [PubMed: 18781835]
13. Rezende RA, Azevedo FS, Pereira FD, Kasyanov V, Wen X, de Silva JVL, et al. Nanotechnological strategies for biofabrication of human organs. J Nanotechnol. 2012; 2012
14. Sasaki T, Iwasaki N, Kohno K, Kishimoto M, Majima T, Nishimura SI, et al. Magnetic nanoparticles for improving cell invasion in tissue engineering. J Biomed Mater Res A. 2007; 86:969–78. [PubMed: 18067168]
15. Shimizu K, Ito A, Arinobe M, Murase Y, Iwata Y, Narita Y, et al. Effective cell-seeding technique using magnetite nanoparticles and magnetic force onto decellularized blood vessels for vascular tissue engineering. J Biosci Bioeng. 2007; 103:472–8. [PubMed: 17609164]
16. Shimizu K, Ito A, Honda H. Mag-seeding of rat bone marrow stromal cells into porous hydroxyapatite scaffolds for bone tissue engineering. J Biosci Bioeng. 2007; 104:171–7. [PubMed: 17964479]
17. Zhang L, Webster TJ. Nanotechnology and nanomaterials: promises for improved tissue regeneration. Nano Today. 2009; 4:66–80.
18. Zhou Y, Li K, Yang JY, Guan CX, Wang Y, Liu CJ, et al. Small-caliber vascular prosthesis prototype based on controlled release of heparin from meso-channels and its enhanced biocompatibility. Small. 2012; 8:1373–83. [PubMed: 22378541]
19. Ito A, Ino K, Kobayashi T, Honda H. The effect of RGD peptide-conjugated magnetite cationic liposomes on cell growth and cell sheet harvesting. Biomaterials. 2005; 26:6185–93. [PubMed: 15899515]
20. Buyukhatipoglu K, Chang R, Sun W, Clyne AM. Bioprinted nanoparticles for tissue engineering applications. Tissue Eng Part C Methods. 2010; 16:631–42. [PubMed: 19769526]
21. Frasca G, Gazeau F, Wilhelm C. Formation of a three-dimensional multicellular assembly using magnetic patterning. Langmuir. 2009; 25:2348–54. [PubMed: 19166275]
22. Muthana M, Scott SD, Farrow N, Morrow F, Murdoch C, Grubb S, et al. A novel magnetic approach to enhance the efficacy of cell-based gene therapies. Gene Ther. 2008; 15:902–10. [PubMed: 18418420]
23. Pislaru SV, Harbuzariu A, Agarwal G, Witt Aas Cvt Latg T, Gulati R, Sandhu NP, et al. Magnetic forces enable rapid endothelialization of synthetic vascular grafts. Circulation. 2006; 114:I-314–318. [PubMed: 16820592]
24. Souza GR, Molina JR, Raphael RM, Ozawa MG, Stark DJ, Levin CS, et al. Three-dimensional tissue culture based on magnetic cell levitation. Nat Nanotechnol. 2010; 5:291–6. [PubMed: 20228788]
25. Akiyama H, Ito A, Kawabe Y, Kamihira M. Cell-patterning using poly (ethylene glycol)-modified magnetite nanoparticles. J Biomed Mater Res A. 2010; 92A:1123–30. [PubMed: 19306262]
26. Jakab K, Neagu A, Mironov V, Markwald RR, Forgacs G. Engineering biological structures of prescribed shape using self-assembling multicellular systems. Proc Natl Acad Sci U S A. 2004; 101:2864–9. [PubMed: 14981244]

27. Berry CC, Wells S, Charles S, Aitchison G, Curtis ASG. Cell response to dextran-derivatised iron oxide nanoparticles post internalisation. Biomaterials. 2004; 25:5405–13. [PubMed: 15130725]
28. Pisanic TR Ii, Blackwell JD, Shubayev VI, Fiñones RR, Jin S. Nanotoxicity of iron oxide nanoparticle internalization in growing neurons. Biomaterials. 2007; 28:2572–81. [PubMed: 17320946]
29. Farrell E, Wielopolski P, Pavljasevic P, van Tiel S, Jahr H, Verhaar J, et al. Effects of iron oxide incorporation for long term cell tracking on MSC differentiation in vitro and in vivo. Biochem Biophys Res Commun. 2008; 369:1076–81. [PubMed: 18336785]
30. Liu JS, Gartner ZJ. Directing the assembly of spatially organized multicomponent tissues from the bottom up. Trends Cell Biol. 2012; 22:683–91. [PubMed: 23067679]
31. Nichol JW, Khademhosseini A. Modular tissue engineering: engineering biological tissues from the bottom up. Soft Matter. 2009; 5:1312–9. [PubMed: 20179781]
32. Dvir-Ginzberg M, Gamlieli-Bonshtein I, Agbaria R, Cohen S. Liver tissue engineering within alginate scaffolds: effects of cell-seeding density on hepatocyte viability, morphology, and function. Tissue Eng. 2003; 9:757–66. [PubMed: 13678452]
33. Mironov V, Zhang J, Gentile C, Brakke K, Trusk T, Jakab K, et al. Designer 'blueprint' for vascular trees: morphology evolution of vascular tissue constructs. Virtual Phys Prototyp. 2009; 4:63–74.
34. Gwyther TA, Hu JZ, Christakis AG, Skorinko JK, Shaw SM, Billiar KL, et al. Engineered vascular tissue fabricated from aggregated smooth muscle cells. Cells Tissues Organs. 2011; 194:13–24. [PubMed: 21252472]
35. Hajdu Z, Mironov V, Mehesz AN, Norris RA, Markwald RR, Visconti RP. Tissue spheroid fusion-based in vitro screening assays for analysis of tissue maturation. J Regen Med Tissue Eng. 2010; 4:659–64.
36. Boland T, Xu T, Damon B, Cui X. Application of inkjet printing to tissue engineering. Biotechnol J. 2006; 1:910–7. [PubMed: 16941443]
37. L'heureux N, Pâquet S, Labbé R, Germain L, Auger FA. A completely biological tissue-engineered human blood vessel. FASEB J. 1998; 12:47–56. [PubMed: 9438410]
38. Mironov V, Visconti RP, Kasyanov V, Forgacs G, Drake CJ, Markwald RR. Organ printing: tissue spheroids as building blocks. Biomaterials. 2009; 30:2164–74. [PubMed: 19176247]
39. Ito A, Ino K, Hayashida M, Kobayashi T, Matsunuma H, Kagami H, et al. Novel methodology for fabrication of tissue-engineered tubular constructs using magnetite nanoparticles and magnetic force. Tissue Eng. 2005; 11:1553–61. [PubMed: 16259609]

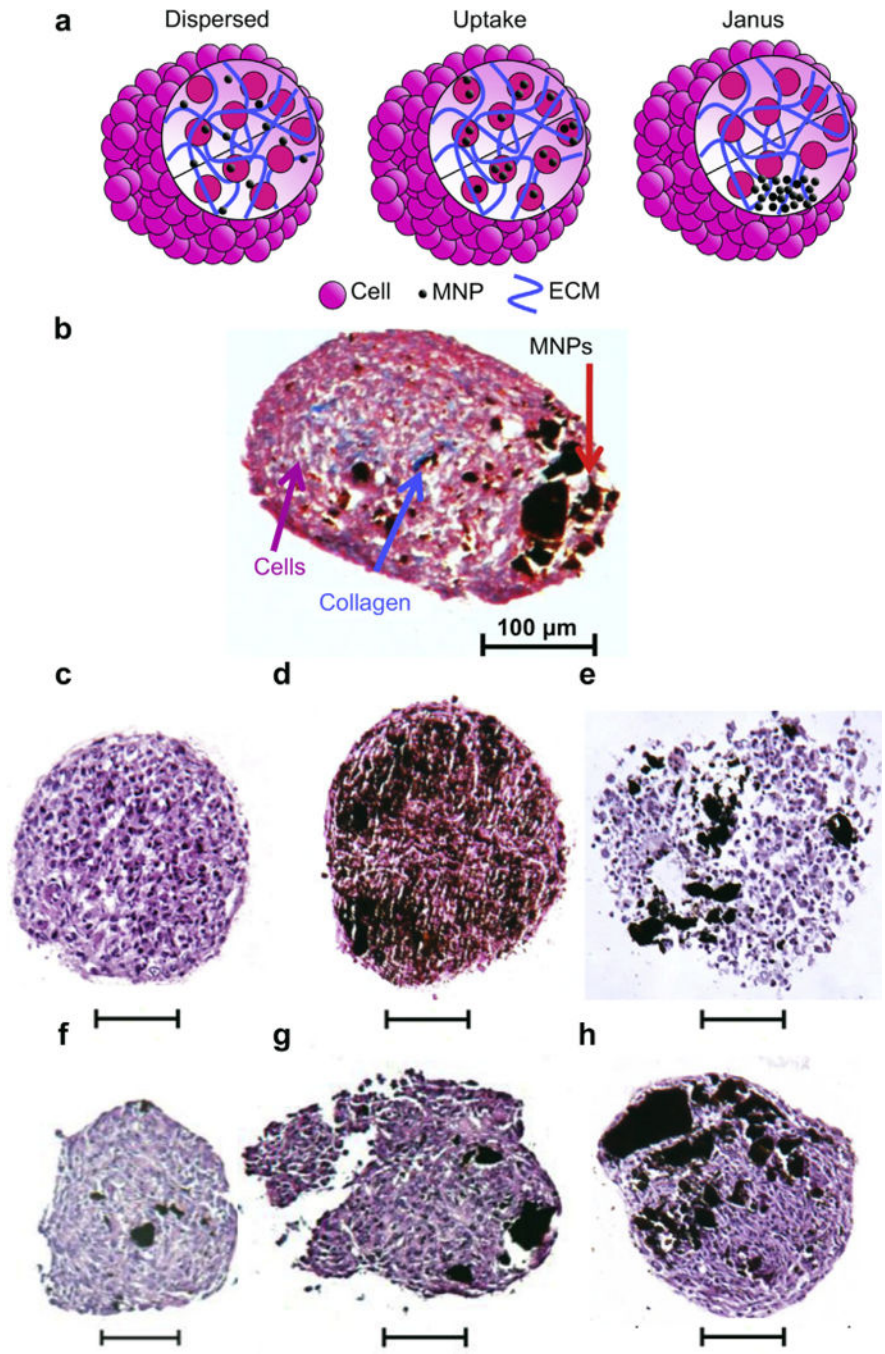

Fig. 1.

Structure of JMCSs. (a) Janus magnetic spheroid structures avoid cytotoxic affects associated with MNP internalization common to dispersed and uptake methods by separating MNPs and cells into segregated and distinct domains. The combination of MNPs (black), cells (pink), and ECM (collagen, blue) into segregated domains decreases cellular toxicity related to MNPs by decreasing interactions with cells. (b) The separation of MNPs and cells is present within JMCSs containing dispersed collagen and primary rat aortic smooth muscle cells with a segregated MNP domain (Masson's Trichrome) (c–h) Analyzed

after three days of assembly, spheroid samples were stained using H&E to confirm the presence and segregation of MNPs within cellular spheroids containing various concentrations of MNPs, (No MNPs = c, increasing MNP concentrations f–h, scale bars = 100 μm). Results confirmed the segregation of MNPs (black) and cells (purple) into distinct domains using multiple MNP concentrations (Janus, f–h). Uptake and dispersed spheroid samples were also stained using H&E (d–e, scale bars = 100 μm). (For interpretation of the references to color in this figure legend, the reader is referred to the web version of this article.)

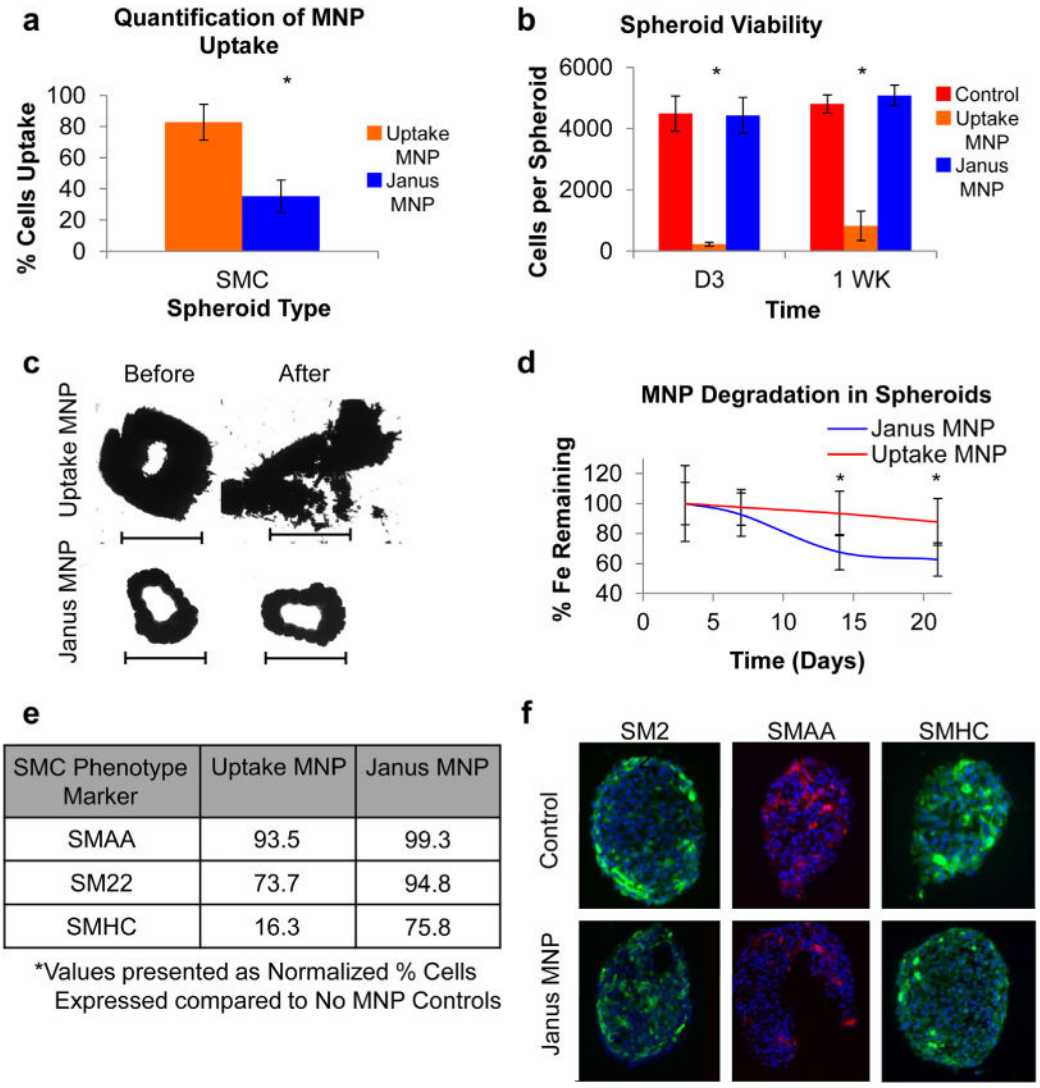

SMC Phenotype Marker	Uptake MNP	Janus MNP
SMAA	93.5	99.3
SM22	73.7	94.8
SMHC	16.3	75.8

*Values presented as Normalized % Cells Expressed compared to No MNP Controls

Fig. 2.

Janus vs. uptake magnetic cellular spheroids. (a) The amount of cells per spheroid that internalized MNPs was quantified and showed that JMCSs (35%) resulted in significantly less MNP internalization than uptake cellular spheroids (83%, $*p < 0.05$). (b) Additionally, cell viability analysis of cellular spheroids fabricated using Janus and uptake methods with primary rat aortic smooth muscle cells revealed that JMCSs maintained high viability compared to control spheroids without MNPs, while uptake spheroids exhibit low viability ($*p < 0.05$) at Days 3 and 7. (c) The use of both spheroid types for tissue engineering applications was analyzed by assembling fused rings via magnetic patterning. After 48 h of fusion, the magnetic patterns were removed and the rings transferred to another chamber. Results showed that rings assembled using uptake spheroids were unable to be physically manipulated and broke apart upon handling. Rings assembled using Janus spheroids, however, were capable of handling, and therefore applicable to tissue engineering applications (scale bars = 1000 μm). (d) The degradation of MNPs within cellular spheroids varied based on the method used to incorporate the MNPs, as results showed 37%

degradation of initial MNP content within JMCSs after 21 days compared to only 12% degradation in uptake MNP spheroids (*$p < 0.05$). (e) SMC phenotype expression of three known SMC markers was quantified using flow cytometry (at least 1 million cells analyzed per sample). Results indicate that JMCSs exhibited similar expression of all three markers compared to controls, while uptake MNP spheroids showed decreased expression of SM22 and SMHC at Day 3. (f) Phenotype expression was qualitatively confirmed using IHC microscopy (red and green = marker, blue = nucleus), confirming uniform dispersion and equivalent expression levels of SMC phenotype markers in JMCSs compared to spheroids without MNP controls. (For interpretation of the references to color in this figure legend, the reader is referred to the web version of this article.)

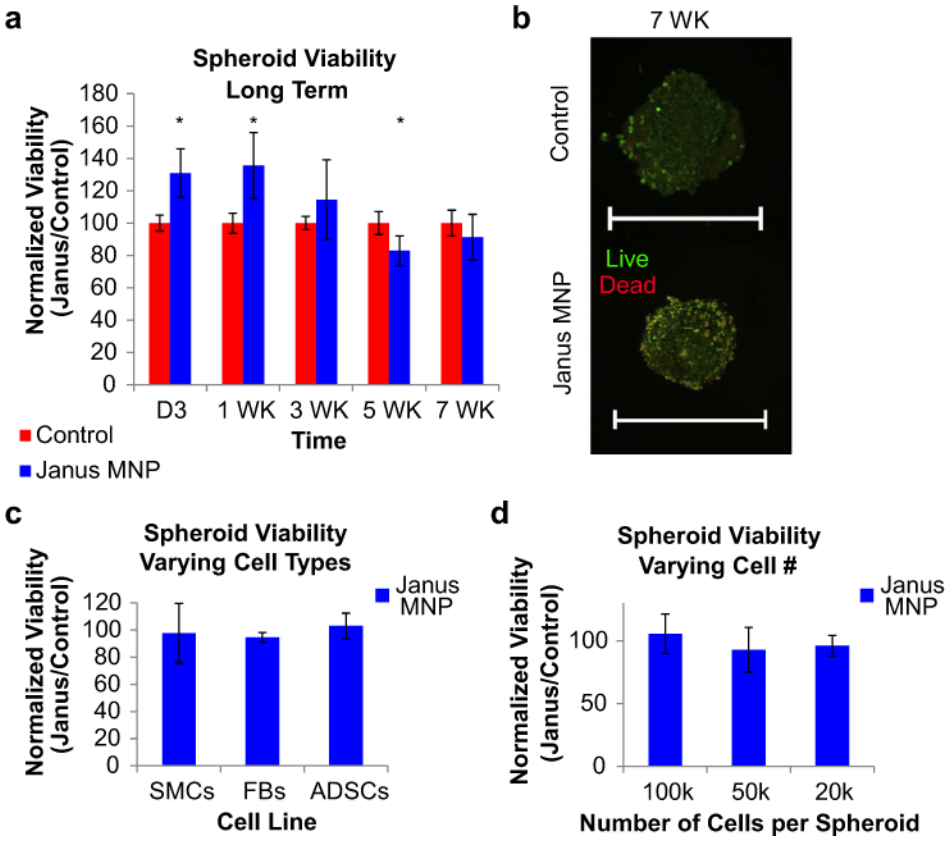

Fig. 3.

JMCS viability – effect of time and spheroid composition. (a,b) Results demonstrated that using Janus magnetic cellular spheroids structures composed of primary rat aortic smooth muscle cells, long term viability was maintained up to 7 weeks, confirmed both quantitatively and qualitatively (confocal microscopy, live/dead stain) compared to control spheroids without MNPs (scale bars = 500 μm). (c) Viability at Day 3 was not affected by cell type, including human adipose-derived stem cells (ADSCs) and rat fibroblasts (FBs) (d) JMCSs were also fabricated with varying cell densities while still maintaining high viability compared to MNP-free controls at Day 3.

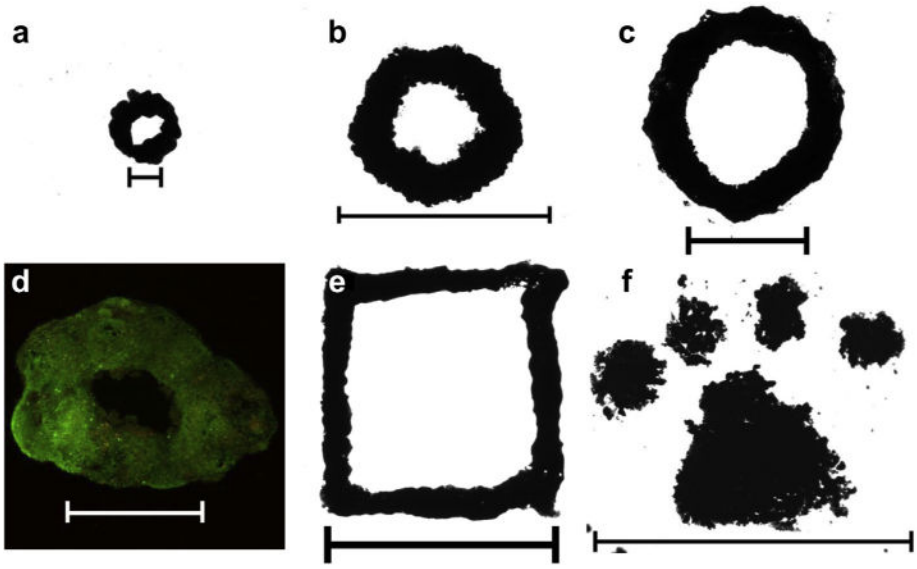

Fig. 4.

JMCSs aligned and fused into homogenous tissues using magnetic patterning. (a–c) JMCSs composed of primary rat aortic smooth muscle cells were patterned and fused together into rings of varying sizes, ranging from 2 mm (a, 25 JMCSs, scale bar = 1000 μm) up to 10 mm (b, c, 3000 JMCSs each, scale bar = 10 mm). (d) Furthermore, viability of the fused structure was confirmed using simultaneous live/dead (green/red) fluorescent staining (scale bar = 1000 μm). (e, f) Finally, using various magnetic patterns, spheroids assembled onto custom patterns can fuse together over the course of days to form fused constructs, demonstrated by a square (e) and Clemson University Tiger Paw (f). Samples shown in images were allowed to fuse over the course of 4 days (scale bars: e = 5 mm, f = 10 mm). (For interpretation of the references to color in this figure legend, the reader is referred to the web version of this article.)

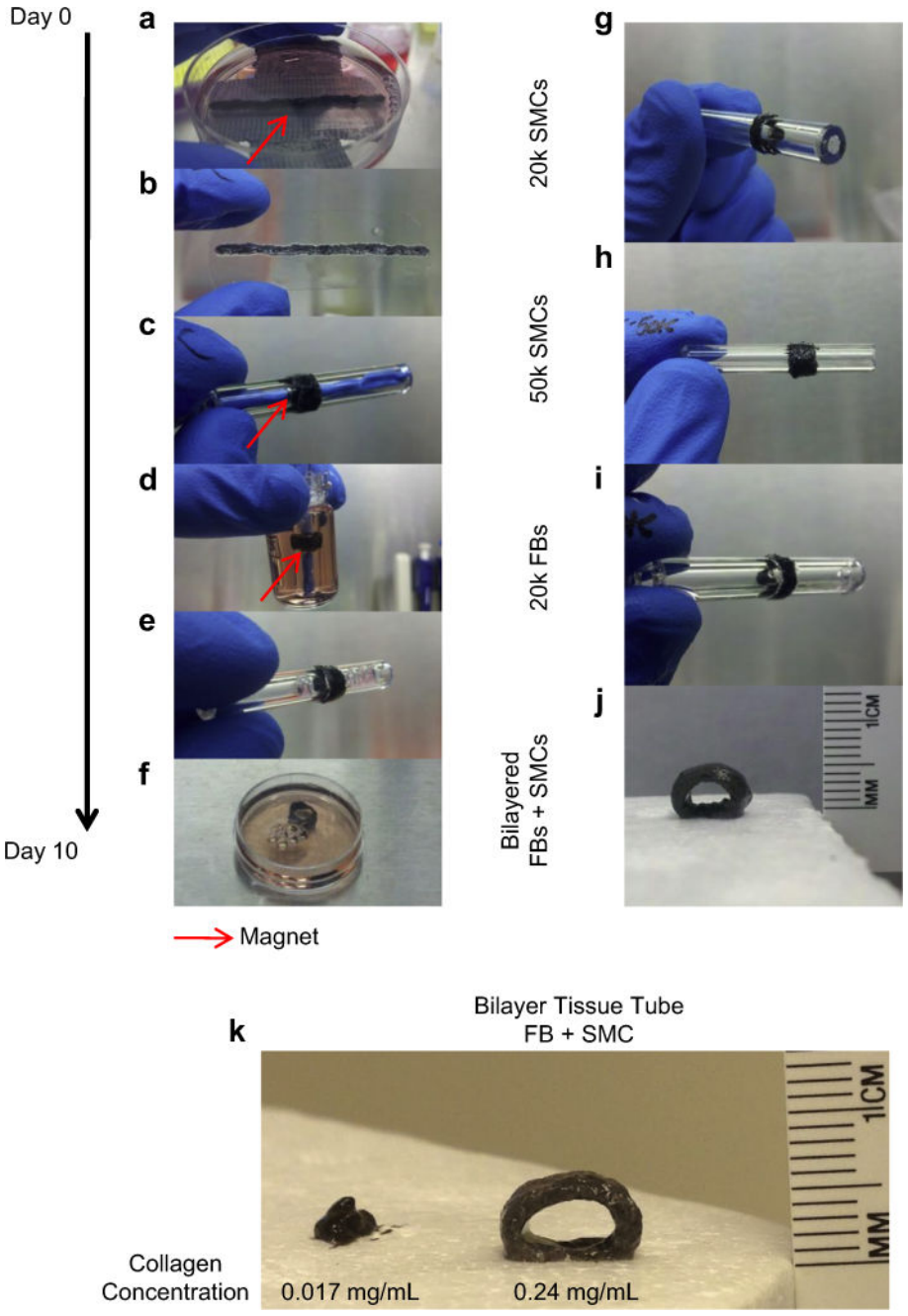

Fig. 5.

Assembly and fabrication of complex tissues. (a) Janus magnetic cellular spheroids composed of primary rat aortic smooth muscle cells were assembled on top of a magnet template, (b) fused into a strip after 4 days, magnet removed, (c, d) wrapped around the glass tube using magnetic attraction, and (e, f) assembled as a fused tube after 6 additional days (10 days total). Additionally, this technique can be expanded for use with: (g, h) varying cell densities, (i) cell types (Fibroblasts, FBs), and (j) even bilayered tubes (0.24 mg/mL collagen I). (k) Bilayer tissue tubes were assembled with high (0.24 mg/mL) and low (0.017 mg/mL) collagen contents to determine the role of collagen in structural support.

Results showed that collagen content plays a critical role in structural integrity, as low collagen tissue tubes collapsed upon removal from the mandrel template, while high collagen tissue tubes remained open and capable of physical handling.

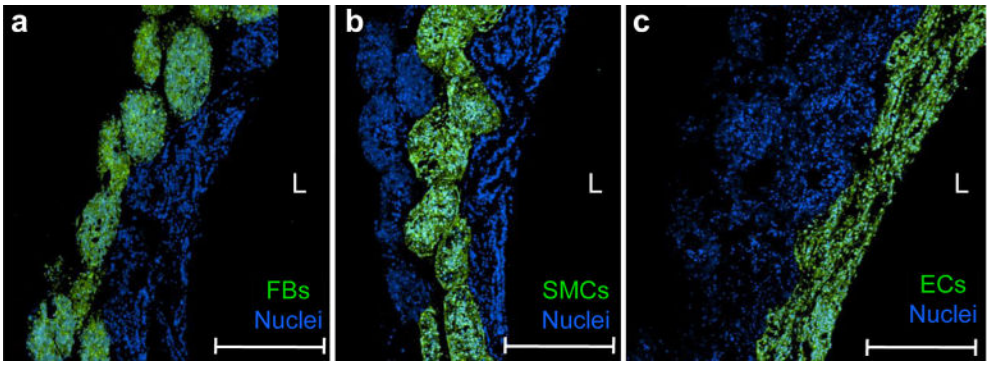

Fig. 6.

Assembly of vascular tissue construct using JMCSs. (a–c) To confirm the presence of three distinct cell types (primary rat aortic ECs, FBs, and SMCs) in different spatial locations, three separate trilayer tubes were assembled and analyzed (L = lumen). For each tube, one cell type was labeled prior to tissue assembly (green). The whole tissue was stained for nuclei to visualize the location of other non-labeled cells and tissue tube boundaries. Results showed that three different cell types could be incorporated into a trilayer tube, demonstrating spatial control over the orientation of each cell type to mimic the native orientation found in vascular tissues. Results indicate that JMCSs can be successfully fabricated into tissue tubes mediated by magnetic forces and incorporate multiple cell types with control over spatial alignment of cells and tissue composition. Scale bars = 500 μm.

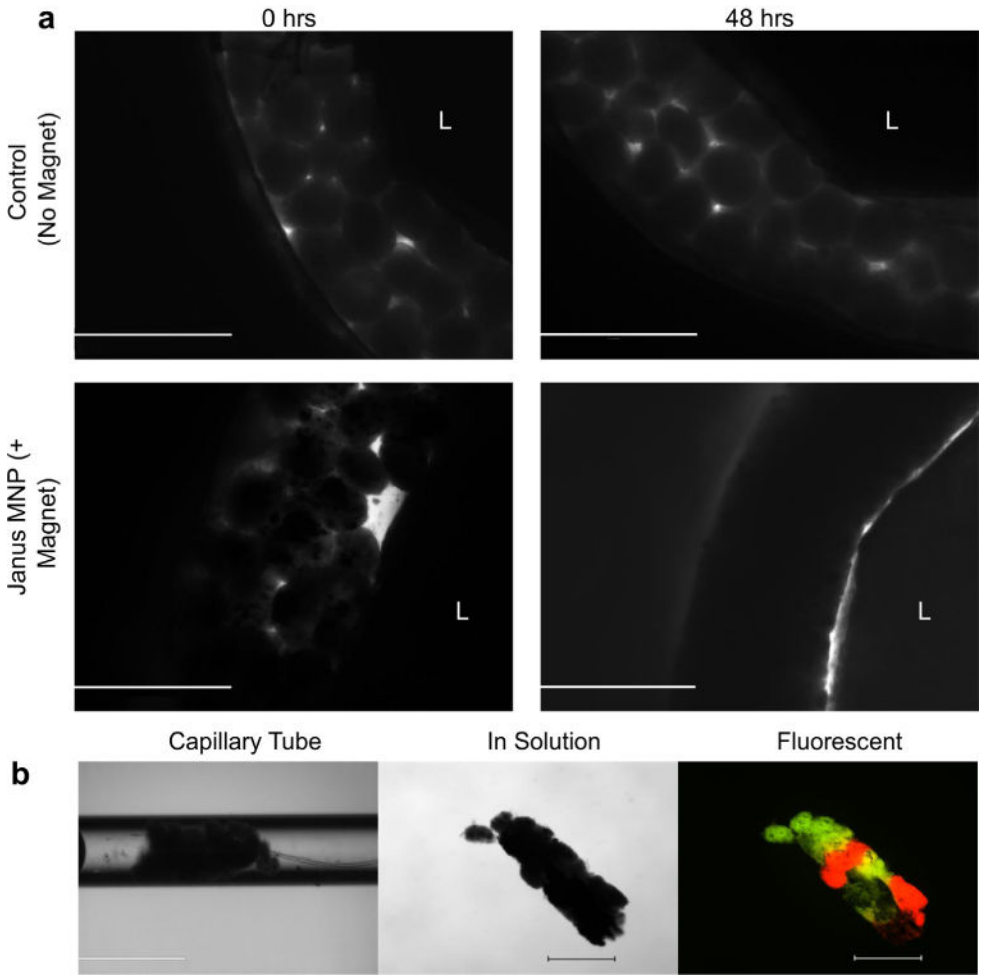

Fig. 7.

Effect of magnetic force application on spheroid fusion. (a) Janus MNP and MNP-free control spheroids (primary rat aortic SMCs) were each seeded into silicone ring molds and allowed to fuse for 48 h. JMCS ring molds were exposed to magnetic forces, while MNP-free control ring molds were not. Results showed that MNP-free control rings experienced minimal fusion, as individual spheroids were visible after 48 h. Results demonstrated that, over 48 h, magnetic forces mediated the fusion of JMCSs into a fused tissue ring. Scale bars = 1000 μm. (b) Fluorescently labeled JMCSs were placed into capillary tubes and then exposed to magnetic forces. After 48 h, results showed a fused tissue construct inside the capillary tube (b, capillary tube). This fused construct could be removed from the capillary tube and handled for imaging (b, in solution). Fluorescent imaging of these spheroids showed that the spatial orientation was maintained throughout the tissue fusion process (b, fluorescent). Scale bars: capillary tube = 1000 μm, in solution and fluorescent = 500 μm.

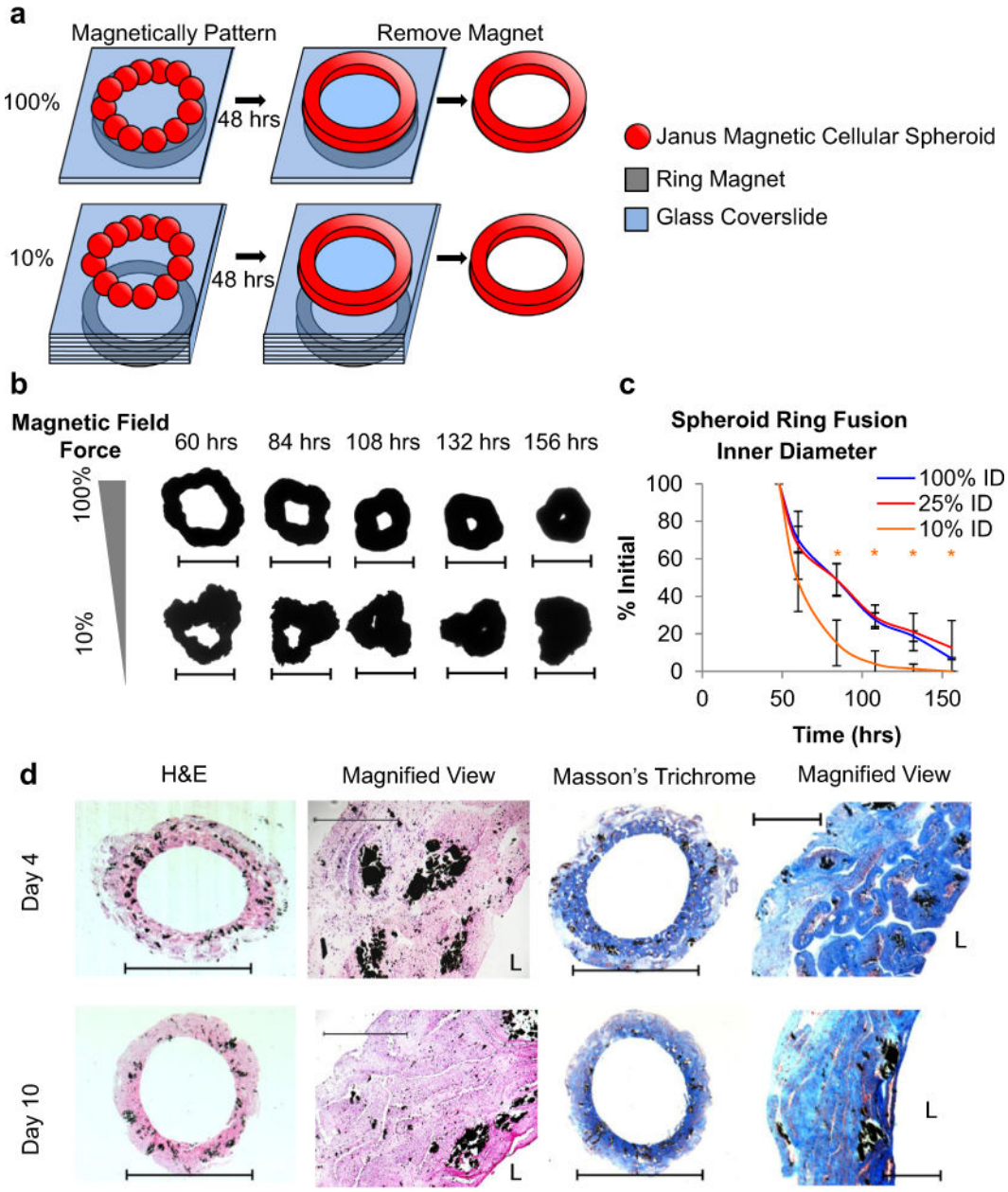

Fig. 8.

Factors affecting JMCS fusion. (a) To study the fusion of JMCSs, twenty five individual JMCSs were magnetically assembled onto a ring magnet. (b, c) Results showed that the strength of the magnet used for JMCS fusion plays a critical role in their fusion into the desired shape. JMCS patterning using a weak magnet (10% of maximum magnetic field) showed a greater rate of inner diameter contraction than those patterned using stronger magnetic fields. All samples using 10% of the maximum field collapsed on themselves. (d) Additionally, tissues tube were assembled using thousands of JMCSs and showed that fusion time is important for tissue assembly, as tissues at Day 4 still presented individual JMCSs

(scale bar = 5 mm, magnified = 500 μm). The H&E stains at Days 4 and 10 confirm the presence of viable cells, as demonstrated by the visualization of nuclei throughout the tissue.